Free Vibrations of Ring-Stiffened Toroidal Shells

THEODORE BALDERES*
Grumman Aerospace Corporation, Bethpage, N.Y.

AND

ANTHONY E. ARMENÀKAS†
Polytechnic Institute of Brooklyn, Brooklyn, N.Y.

In this investigation, the free vibrations of ring-stiffened toroidal shells are studied. The stiffening rings which are placed at meridional sections are treated as discrete members, each with different properties and unequally spaced. The shell is broken up into shell segments whose motion is studied on the basis of the Love-Reissner shell theory. Stiffness matrices for the shell segments are obtained by expanding the shell parameters in the meridional direction and integrating numerically in the circumferential direction. The stiffness matrices of the reinforcing rings are combined with those of the shell segments by imposing compatibility at the junctions. This results in a set of linear homogeneous algebraic equations which are solved by a fast converging iteration technique. A comparison of the frequencies of unstiffened toroidal shells shows good concurrence with available results. Plots are established showing the effect of the shell parameters on the frequencies of the unstiffened shells. The results indicate that the frequencies increase with increasing ζ (thickness to radii ratio, h/R) and decreasing η (radii ratio, a/R). The five lowest frequencies and their corresponding mode shapes are determined for three different cases. When stiffening rings are added to the toroidal shells, the frequencies either remain the same or increase substantially. The changes being greater for shells with smaller η. Moreover, the presence of additional modes is established as well as the coupling of circumferential harmonics.

Nomenclature

a	= distance between center of the cross section and the axis of revolution of a toroidal shell
h	= thickness of the shell
m, n	= Fourier indices
r	= radius of parallel circle
r_1, r_2	= meridional and circumferential radii of curvature
R	= radius of circular cross section of a toroidal shell, radius of the ring stiffener
t	= time
u, v, w	= circumferential, meridional and radial displacement components of a point on the middle surface of the shell
z	= coordinate normal to middle surface of the shell
θ, Ψ	= circumferential and meridional coordinates of the toroidal shell
$\bar{A} = A/R$	= nondimensional cross sectional area of a ring stiffener
E, E_r	= modulus of elasticity of the shell, and the stiffeners, respectively
$\bar{E} = E_r/E$	= nondimensional modulus of elasticity of the stiffeners
G, G_r	= shear modulus of the shell, and the stiffeners, respectively
$\bar{G} = G_r/E$	= nondimensional shear modulus of the stiffeners
$\bar{I}_\psi = I_\psi/R^4$	= in plane; nondimensional moments of inertia of the stiffeners
$\bar{I}_z = I_z/R^4$	= out of plane; nondimensional moments of inertia of the stiffeners
$\bar{J} = J/R^4$	= nondimensional torsional constant of the stiffeners
η	= radii ratio (a/R)
ζ	= thickness to radius ratio (h/R)
λ	= $\rho\Omega^2 a^2/E$
ν	= Poisson's ratio
ρ	= density
Ω	= circular frequency
ω_ψ	= rotational displacement about ψ direction

Received January 23, 1973; revision received July 27, 1973. This paper is based upon part of a dissertation by T. Balderes submitted in partial fulfillment of the requirements for the Ph.D. degree (Applied Mechanics) to the Polytechnic Institute of Brooklyn, June 1972. The investigation was partly supported by the Air Force Office of Scientific Research under Contract F44620-C-0072, Project 9782-01 with the Polytechnic Institute of Brooklyn. The authors wish to acknowledge A. Liepins' assistance in providing numerical results for unstiffened shells for comparison.

Index category: Structural Dynamic Analysis.

* Structural Mechanics Engineer. Associate Member AIAA.

† Professor of Applied Mechanics, Department of Aerospace Engineering and Applied Mechanics. Associate Fellow AIAA.

Introduction

STUDIES of toroidal shells have dealt with the static, dynamic and buckling analysis of torus sectors and of complete unstiffened toroidal shells. Among some of the more recent studies, are those of Sanders and Liepins[1] who considered the toroidal membrane under uniform normal pressure. An extension of their approach using both the nonlinear membrane theory and the bending theory was presented by Rossettos and Sanders.[2] Reissner[3] also investigated this problem and ascertained when the linear bending, the nonlinear membrane, or the nonlinear bending theory should be employed.

In a series of papers,[4-5] Liepins studied the free vibrations of prestressed toroidal shells. The analysis was based on a linearized theory of prestressed shells, and utilized Fourier series expansions in the circumferential direction and finite difference approximations in the meridional direction. The membrane theory was used in the first paper, whereas, in the second investigation, the effects of bending stiffness were considered. It was established that the flexural modes are altered considerably with the addition of bending stiffness.

A study concerned with both buckling and vibrations of toroidal shells was presented by Flügge and Sobel.[6] Equations governing buckling and free vibrations of prestressed thin shells of revolution were derived and were then applied to the analysis of toroidal shells. The stability equations were solved by the use of Fourier series expansions in the circumferential and meridional directions. Design curves giving the buckling pressures for a wide range of geometric parameters were presented.

In this investigation the free vibrations of ring-stiffened toroidal shells are studied. The stiffening rings which are assumed placed at meridional sections, are treated as discrete members (Fig. 1). The shell segments, whose motion is analyzed on the

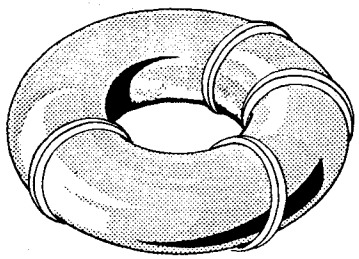

Fig. 1 Ring-stiffened toroidal shell.

basis of the Love-Reissner shell theory, are coupled to the stiffeners by imposing compatibility at the junctions. Thus, in the present analysis, the influence of an arbitrary number of rings, differing in properties and unequally spaced can be considered.

Governing Equations

The geometry and notation for a toroidal shell with a circular meridian is shown in Fig. 2. The radius of curvature of the meridian is denoted by R and the distance between the center of the circular cross section and the axis of revolution is denoted by a. The radius of curvature in the circumferential direction r_2 is given by

$$r_2 = AP = a/\cos\Psi + R \tag{1}$$

and the distance r is

$$r = r_2\cos\Psi = a + R\cos\Psi \tag{2}$$

The lines of principal curvature are the meridians (θ = const) and the parallel circles (Ψ = const) as shown in Fig. 2. Accordingly, the angles θ and Ψ and the distance from the middle surface z, are used as the coordinate system.

The components of displacement $\bar{u}$, $\bar{v}$, $\bar{w}$ at the middle plane of the shell are expressed as

$$\begin{aligned}\bar{u}(\theta,\Psi,t) &= u(\theta,\Psi)\cos\Omega t\\ \bar{v}(\theta,\Psi,t) &= v(\theta,\Psi)\cos\Omega t\\ \bar{w}(\theta,\Psi,t) &= w(\theta,\Psi)\cos\Omega t\end{aligned} \tag{3}$$

They are taken positive in the directions of increasing θ, Ψ, and z. The natural boundary conditions for the edges of a sector of the shell $\theta = \theta_1$ and $\theta = \theta_2$ are

a) u or N_θ is prescribed

b) v or $T_{\Psi\theta} = N_{\Psi\theta} - (M_{\Psi\theta}/R)$ is prescribed

c) w or $J_\theta = Q_\theta + (1/R)(\partial/\partial\Psi)(M_{\Psi\theta})$ is prescribed

d) ω_Ψ or M_θ is prescribed (4)

where N_θ, $T_{\Psi\theta}$, J_θ and M_θ are referred to as the effective stress resultants.

The displacement equations of motion of a sector of the toroidal shell may be converted into a set of eight partial differential equations with variable coefficients, expressing the first derivatives with respect to θ of the eight shell functions u, v, w, ω_Ψ, N_θ, $T_{\Psi\theta}$, J_θ and M_θ appearing in the natural boundary conditions of a meridional section.[7] The resulting equations are of the form

$$\frac{\partial y_i}{\partial\theta} = \sum_{j=1}^{8}\left\{a_{ij}y_j + b_{ij}\frac{\partial y_j}{\partial\Psi} + c_{ij}\frac{\partial^2 y_j}{\partial\Psi^2} + d_{ij}\frac{\partial^3 y_j}{\partial\Psi^3}\right\} \tag{5}$$

$$(i = 1,2,\ldots 8)$$

where y_i denotes one of the eight shell functions. Their coefficients are functions of the shell geometry and the shell properties. Inasmuch as some of these coefficients involve powers of the trigonometric functions, in order to facilitate the subsequent Fourier series analysis, these coefficients are expressed as linear combinations of trigonometric functions by using appropriate trigonometric identities.[7]

For a toroidal shell with a closed meridian, the condition of periodicity of the shell functions is satisfied if the shell functions are expanded in the following Fourier series expansions in the meridional direction

$$y_i = \sum_{m=0}^{\infty} Y_{mi}\cos m\Psi + \sum_{m=1}^{\infty} Y_{mi}'\sin m\Psi \tag{6}$$

The series with the unprimed coefficients represents motion which is symmetric about the plane $\Psi = 0$, $\Psi = \pi$, whereas, the series with the primed coefficients represents motion that is antisymmetric about this plane. By substituting expressions (6) into Eqs. (5), it can be shown that the resulting equations may be written in the form

$$\sum_{m=0}^{\infty}\frac{dY_{mi}}{d\theta}\cos m\Psi + \sum_{m=1}^{\infty}\frac{dY_{mi}'}{d\theta}\sin m\Psi = \sum_{m=0}^{\infty}A_{mi}\cos m\Psi + \sum_{m=1}^{\infty}A_{mi}'\sin m\Psi \tag{7}$$

$$(i = 1,2,\ldots 8)$$

The quantities Ami and $A'mi$ are functions of the coefficients of Ymi and $Y'mi$, respectively.

Since the functions $\cos m\Psi$ and $\sin m\Psi$ are linearly independent in the interval $0 \leqq \Psi \leqq 2\pi$, the symmetric and antisymmetric motions of the torus are uncoupled. Equations (7) then represent two sets of uncoupled equations which can be treated separately.

Symmetric Motion

For motion that is symmetric about the plane $\Psi = 0$, $\Psi = \pi$, substitution of the first part of the Fourier series expansions (6) into Eqs. (5), results in a set of eight equations involving terms which consist of products of trigonometric functions and Fourier series. The first of these equations is of the following form:

$$\begin{aligned}\sum_{m=0}^{\infty}\frac{du_m}{d\theta}\cos m\Psi = a_{11}\sin\Psi\sum_{m=1}^{\infty}v_m\sin m\Psi +\\ (a_{20}+a_{21}\cos\Psi)\sum_{m=1}^{\infty}mv_m\cos m\Psi +\\ (a_{30}+a_{31}\cos\Psi)\sum_{m=0}^{\infty}w_m\cos m\Psi +\\ (a_{40}+a_{41}\cos\Psi)\sum_{m=0}^{\infty}N_{\theta m}\cos m\Psi\end{aligned} \tag{8}$$

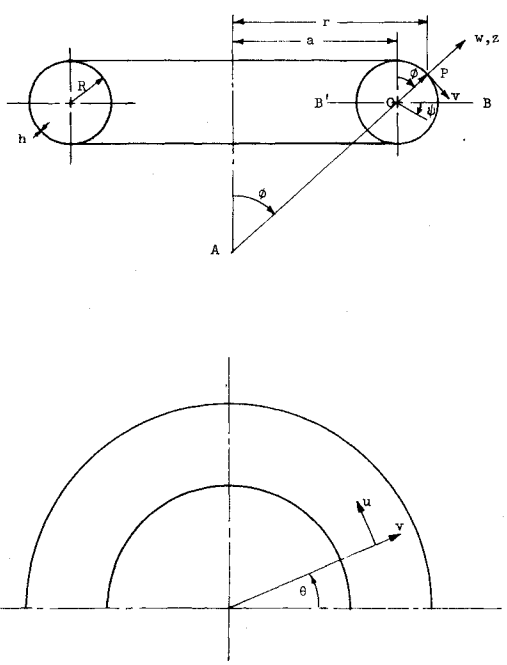

Fig. 2 Geometry and notation for toroidal shell.

where u_m, v_m, w_m, $N_{\theta m}$ denote the amplitudes Y_{m1}, Y_{m2}, Y_{m3}, Y_{m5}, respectively, of the Fourier series expansions (6).

Using certain identities,[7] every term of the aforementioned eight equations may be written as an infinite sum over the same range of m, of the same trigonometric function. Hence, each of the eight equations may be written in the form

$$\sum_{m=0}^{\infty} \frac{dY_{mi}}{d\theta} \cos m\Psi = \sum_{m=0}^{\infty} A_{mi} \cos m\Psi$$

or

$$\sum_{m=1}^{\infty} \frac{dY_{mi}}{d\theta} \sin m\Psi = \sum_{m=0}^{\infty} A_{mi} \sin m\Psi \tag{9}$$

Since the trigonometric functions $\cos\Psi$, $\cos 2\Psi$, $\cos 3\Psi \ldots$, $\sin\Psi$, $\sin 2\Psi$, $\sin 3\Psi \ldots$ are linearly independent in the range $0 \leqq \Psi \leqq 2\pi$, each of the eight equations yields an infinite number of equations, one for each value of m.

Thus, we obtain an infinite number of sets of eight or less ordinary differential equations with constant coefficients. Each set expresses the derivatives of the eight amplitudes in Eq. (6) corresponding to the same value of m (harmonic). In these relations the various harmonics are coupled unlike the case of axisymmetric shells of revolution where the harmonics are not coupled and may be considered separately in vibration analysis.[8]

Antisymmetric Motion

For motion that is antisymmetric about the plane $\Psi = 0$ and $\Psi = \pi$, substituting the second part of the Fourier expansions (6) into Eqs. (5) and following the same procedure as in the symmetric case, an infinite number of sets of eight or less ordinary differential equations governing the antisymmetric motion are obtained.[7]

Computation of Influence Coefficients

The influence coefficients for the toroidal shell segments are obtained by retaining a finite number, N, of the infinite number of sets of the equations for the symmetric and antisymmetric motion and employing a numerical integration procedure. In some equations, terms with higher harmonics than $m = N-1$ exist; these harmonics are omitted for consistency. That is, the first $m = 0, 1, 2, \ldots N-1$ harmonics are retained in the resulting N sets of equations. For example, if only the $m = 0$ and $m = 1$ harmonics for the symmetric motion are retained, we obtain an $m = 0$ set of equations involving only $m = 0$ and $m = 1$ harmonics, which is of the form

$$\frac{dY_{0i}}{d\theta} = \sum_{j=1}^{8} A_{0j}^{(0)} Y_{0j} + \sum_{j=1}^{8} A_{1j}^{(0)} Y_{1j} \tag{10a}$$

and an $m = 1$ set of equations involving only $m = 0$ and $m = 1$ harmonics

$$\frac{dY_{1i}}{d\theta} = \sum_{j=1}^{8} A_{0j}^{(1)} Y_{0j} + \sum_{j=1}^{8} A_{1j}^{(1)} Y_{1i} \tag{10b}$$

$$(i = 1, 2 \ldots 8)$$

Similar sets are obtained for the antisymmetric motion. It should be noted that the derivatives $(d/d\theta)(N_{\theta 0})$ and $(d/d\theta)(N_{\theta 1})$ are coupled in the aforementioned equations. Generally, in applying the stepwise integration procedure to shells of other geometries[8] coupling of the derivatives of a shell function does not occur.

Integration of Eqs. (10) is carried out by using a Runge-Kutta fifth-order formula which is given in Ref. 7. The integration procedure commences by assuming a unit value for one of the functions u_0, w_0, $\omega_{\Psi 0}$, u_1, v_1, w_1, $\omega_{\Psi 1}$, $N_{\theta 0}$, $J_{\theta 0}$, $M_{\theta 0}$, $N_{\theta 1}$, $T_{\Psi\theta 1}$, $J_{\theta 1}$, or $M_{\theta 1}$ at one end of the shell segment ($\theta = \theta i$), while setting all the others to zero. By using the Runge-Kutta numerical integration technique,[7] the values of the functions at the other end of the shell segment ($\theta = \theta j$) are computed. This procedure yields the following relations:

$$\begin{aligned} \{F_j\} &= [X_1]\{\Delta_i\} + [X_2]\{F_i\} \\ \{\Delta_j\} &= [Y_1]\{\Delta_i\} + [Y_2]\{F_i\} \end{aligned} \tag{11}$$

Where the terms of the vector $\{F_j\}$ are the harmonics of the stress resultants $N_{\theta 0}$, $J_{\theta 0}$, $M_{\theta 0}$, $N_{\theta 1}$, $T_{\Psi\theta 1}$, $J_{\theta 1}$, and $M_{\theta 1}$ at edge j, whereas, the terms of the vector $\{\Delta_j\}$ are the harmonics of the shell displacements u_0, w_0, $\omega_{\Psi 0}$, u_1, v_1, w_1 and $\omega_{\Psi 1}$ at edge j. The elements of the matrices $[X_1]$, $[X_2]$ and $[Y_1]$ and $[Y_2]$ are the influence coefficients for the shell segment.

Firstly, it should be noted, that in order to integrate Eqs. (10) a value for the frequency (Ω) must be assumed since it appears on the right-hand side of the equations. If the frequency is taken as zero, the influence coefficients and the resulting stiffness matrix will describe the static characteristics of the shell segment, while, if a value other than zero is used, the influence coefficients and the stiffness matrix will include the inertia effects. Secondly, it should be noted, there is a restriction on the length of the shell segments. The length of each segment should not be larger than a critical length for which computer roundoff errors become pronounced.

The stiffness matrix for the shell segment is obtained by solving for $\{F_i\}$ and $\{F_j\}$ in Eq. (11). This yields the following:

$$\begin{Bmatrix} F_i \\ F_j \end{Bmatrix} = \left[\begin{array}{c|c} -[Y_2]^{-1}[Y_1] & [Y_2]^{-1} \\ \hline [X_1]-[X_2][Y_2]^{-1}[Y_1] & [X_2][Y_2]^{-1} \end{array}\right] \begin{Bmatrix} \Delta_i \\ \Delta_j \end{Bmatrix} \tag{12}$$

The stiffness matrix for the reinforcing rings which is derived in Ref. 7 is of the form

$$\{F_j\} = [K_R]\{\Delta_j\} \tag{13}$$

Solution of the Equations Governing the Motion of a Ring-Stiffened Toroidal Shell

The stiffness matrix of the complete ring-stiffened toroidal shell is obtained by combining the stiffness matrices of the shell segments and the rings.[7] Addition of the shell and ring stiffness matrices using the direct stiffness method is equivalent to satisfying the following boundary conditions at each junction

$$\begin{aligned} \{F\}_{\text{external}} &= \{F\}_{\text{shell}} + \{F\}_{\text{ring}} \\ \{\Delta\}_{\text{shell}} &= \{\Delta\}_{\text{ring}} \end{aligned} \tag{14}$$

The resulting matrix $[K]$, which relates the amplitudes of the meridional harmonics of the stress resultants to the amplitudes of the meridional harmonics of the displacements at the junctions of the shell segments, includes the effects of the inertia terms. Thus, the governing equations for the motion of a ring-stiffened toroidal shell are given as

$$\{F\} = [K]\{\Delta\} \tag{15}$$

For free vibrations, the governing equations become

$$\{0\} = [K]\{\Delta\} \tag{16}$$

This is a set of M linear algebraic equations; their solution yields M frequencies and M different vibrational patterns corresponding to the M degrees of freedom allowed in the analysis of the shell. That is, every shell segment has $2S$ degrees of freedom depending on the number of harmonics S included in the analysis.‡ If the shell is subdivided into V segments, the total number of degrees of freedom M is given by

$$M = (S)(V)$$

A solution of Eq. (16) can be obtained by employing either of two methods: the determinant method, or an iterative eigenvalue method. In the determinant method values of the frequency are sought which cause the determinant of the coefficients of the Δ's to vanish. This is accomplished by a trial and error procedure. The second method,[9] has certain definite advantages over the determinate approach and is employed in this investigation. The problem of skipping roots which are close together does not exist; moreover, when one eigenvalue is obtained, satisfactory estimates of many other eigenvalues are also available.

‡ If the zero harmonic is only included ($m = 0$) each shell segment has six degrees of freedom, the three harmonics u_0, w_0, $\omega_{\Psi 0}$, at each end. If the zero and first harmonics are included, each segment has fourteen degrees of freedom, the seven harmonics u_0, w_0, $\omega_{\Psi 0}$, u_1, v_1, w_1, $\omega_{\Psi 1}$ at each end.

The problem is cast into the linear eigenvalue form by splitting the stiffness matrix in Eq. (16) into two parts. The first part is the standard elastic stiffness matrix $[K_0]$, obtained by setting the frequency to zero. The second part $[K_1]$ represents the change in the stiffness due to the dynamic effects and is obtained by simply subtracting $[K_0]$ from $[K]$, thus

$$[K_1] = [K] - [K_0] \tag{17}$$

Note that the functional dependence of $[K_1]$ on the frequency is not explicitly defined. Hence, $[K_1]$ can only be formed for a given specific value of Ω. Thus, to form $[K_1]$, a value of the frequency $\Omega = \Omega_{i-1,k}$ is assumed. Having formed $[K_0]$, the solution of Eq. (16) can be formulated as a linear eigenvalue problem requiring an iterative solution.

$$\{[K_0] + \lambda_{ik}{}^2[K_1(\Omega^2_{i-1,k})]\}\{\Delta\} = \{0\} \tag{18}$$

$\lambda_{ik}{}^2$ are the eigenvalues obtained by solving Eq. (18). These eigenvalues can be considered as squares of frequency ratios $(\Omega_{i,k}/\Omega_{i-1,k})^2$. Thus, a new estimate of the frequency is obtained by multiplying the assumed frequency $\Omega_{i-1,k}$ by λ_{ik}. If Eq. (18) is of order M, for each solution, M ratios λ_{ik} $(k = 1, 2 \ldots M)$ are obtained. Each ratio corresponds to one of the free vibration patterns included in the analysis. The ratio corresponding to the desired frequency is selected (if the third frequency is sought the third ratio is taken) and the assumed frequency is multiplied by this ratio, resulting in a new estimate $\Omega_{i,k}$ of the desired frequency Ω_k. Using this new value of $\Omega_{i,k}$, the matrix $[K_1(\Omega_{i,k})]$ is computed and Eqs. (18) are solved again for the M ratios $\lambda_{(i+1)k}$. This process is repeated until the ratio λ_{ik} corresponding to the desired frequency is equal to unity. This indicates that for the assumed value $\Omega_{l-1,k}$ of frequency, the set of Eqs. (18) is identically satisfied and, hence $\Omega_{l-1,k}$ is the desired frequency Ω_k.

The frequencies and vibration patterns obtained by solving the governing Eqs. (16) with either of the two methods described will constitute an estimate of the actual frequencies and vibration patterns of the toroidal shell. The final solution for the frequencies and vibration patterns will be obtained by successively retaining more sets of harmonics, until the results obtained on the basis of m harmonics differ from those obtained on the basis of $m+1$ harmonics by a prescribed error.

A computer program was written that generates the stiffness matrices of the shell segments and rings. This program is described in detail in Ref. 10. The stiffness matrices of the shell segments and rings were combined using a matrix manipulation program.

In order to obtain accurate solutions, the lengths of the toroidal shell segments must not exceed a certain maximum size. Thus, many small shell segments must be joined together to form the entire shell resulting in a very large eigenvalue problem which may exceed computer capacity. To circumvent this difficulty, the Guyan reduction technique[10] is employed to eliminate some of the degrees of freedom.

The eigenvalues and eigenvectors of the reduced eigenvalue problem are obtained by applying the Householder technique. In order to obtain the lowest roots within acceptable accuracy, it is necessary to reduce the $[K_0]$ matrix to triangular form. This requires removal of the rigid body modes, inasmuch as their presence renders the stiffness matrix singular and, consequently, nonreducible. A means of rectifying this difficulty is presented in Ref. 11 where a coordinate transformation is utilized to remove the singularities of $[K_0]$. In this approach, the principle of conservation of momentum is employed in conjunction with equilibrium equations which are rather cumbersome. Another method utilized to remove the singularities of $[K_0]$ is the method of shifts.[10] This method which yields accurate results was employed in this investigation. Consider the eigenvalue problem

$$[K_0]\{\Delta\} = \lambda[K_1]\{\Delta\} \tag{19}$$

In the method of shifts the eignevalues λ, are expressed as

$$\lambda = \lambda^* - \lambda^o \tag{20}$$

where λ^o is a chosen number. Substitution of Eq. (20) into Eq. (19) yields

Table 1 Comparison of frequencies for a toroidal shell with $\eta = 20/3$, $\zeta = 0.01$, $\nu = 0.3$

Symmetric motion

No. of root	n	Frequency λ present investigation	λ Frequency Ref. 5	% Difference
11	2	0.338	0.337	0.3
12	0	0.351	0.346	1.4
18	2	0.383	0.384	0.3
20	0	0.392	0.392	0

Antisymmetric motion

No. of root	n	Frequency λ present investigation	λ Frequency Ref. 5	% Difference
2	0	0.00967	0.0097	0.3
12	2	0.285	0.283	0.7
16	2	0.382	0.374	2.1
18	0	0.386	0.385	0.2

$$\{[K_0] + \lambda^o[K_1]\}\{\Delta\} = \lambda^*[K_1]\{\Delta\} \tag{21}$$

the matrix $\{[K_0] + \lambda^o[K_1]\}$ is not singular and may be reduced to triangular form, and the eigenvalues λ^* can be established. Finally, the eigenvalues λ are obtained from Eq. (20).

Numerical Results for Unstiffened Toroidal Shells

In Table 1, the frequencies obtained in this investigation for a toroidal shell with $\eta = a/R = 20/3$, $\zeta = h/R = 0.01$ and $\nu = 0.3$, are compared with those reported in Ref. 5. The number of a root indicates its relative magnitude. The lowest root is number one. It is noted, that the maximum difference between the two sets of frequencies is 2.1%. This difference may be due to the fact that in Ref. 5, a shell theory presented by Sanders[12] was utilized whereas, in this investigation, the Love-Reissner theory was employed.

It should be noted that the convergence of the iterative linear eigenvalue formulation is very rapid. In all cases, after the first trial only one additional solution was required to obtain each root to four-figure accuracy. Moreover, the formulation employed herein yields the frequencies in ascending order commencing with the lowest, thus eliminating the problem of identifying the roots, a difficulty encountered in the determinant method.[5]

Figure 3 indicates the number of the highest harmonic which must be retained for different values of the shell parameters, in

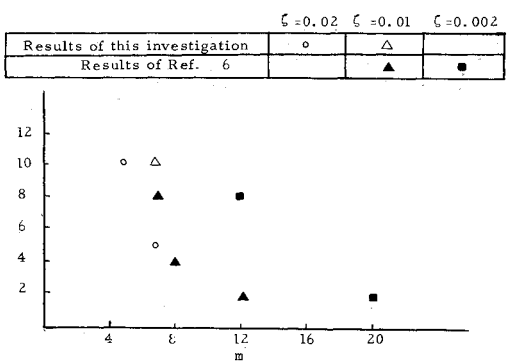

Fig. 3 Number of highest harmonic m that must be retained for convergence to the first root for various values of η and ζ.

Table 2 Frequencies (λ) of unstiffened toroidal shells

	$\eta = 10$		$\zeta = 0.01$		$\eta = 10$		$\zeta = 0.02$		$\eta = 5$		$\zeta = 0.02$
n^a	Symmetric motion	n	Antisymmetric motion	n	Symmetric motion	n	Antisymmetric motion	n	Symmetric motion	n	Antisymmetric motion
2	0.00220	2	0.00256	2	0.00442	2	0.00506	2	0.00901	2	0.00916
3	0.0136	3	0.0141	3	0.0288	3	0.0296	3	0.0378	0	0.0150
4	0.0308	0	0.0148	4	0.0696	0	0.0315	4	0.0752	3	0.0369
5	0.0507	4	0.0308	5	0.122	4	0.0697	5	0.131	4	0.0747
6	0.0763	5	0.0506	6	0.191	5	0.121	6	0.210	5	0.131

[a] n = number of circumferential waves.

order that three-figure accuracy is assured in the eigenvalues. In the same figure the convergence characteristics of the results in Ref. 6 are illustrated. In this reference, the buckling of toroidal shells was investigated. All of the curves pertain to the lowest buckling mode or the lowest eigenvalue of the toroidal shell. The convergence characteristics of the present formulation are analogous to those of Ref. 6. Figure 3 indicates that more harmonics are necessary for the representation of the motion of the toroidal shell as ζ and η decrease. For small values of ζ, the bending stiffness of the shell is small and the mode shapes tend to have more oscillations around the meridian, thus necessitating additional harmonics for accurate representation of the motion. On the other hand, as η increases and in the limit as $\eta \to \infty$, the geometry of the torus approaches that of an infinitely long circular cylinder. Thus, mode shapes of the meridians of the vibrating shell resemble more and more those of the cross section of an infinite cylinder which are represented by harmonic functions. Due to the increase in the circumferential curvature, the mode shapes along the meridians of toroidal shells with small η values become more and more distorted from the regular harmonic shapes. Consequently, additional harmonics are required to represent accurately the mode shapes of the shell.

Table 2 gives the five lowest frequencies of the symmetric and antisymmetric motion for three different toroidal shells. For all cases considered, the lowest eigenvalue for both the symmetric and the antisymmetric motion, corresponds to motion involving two circumferential waves ($n = 2$). For the symmetric motion the next four roots correspond to three, four, five and six circumferential waves ($n = 3, 4, 5, 6$). For antisymmetric motion in the first two cases, the third mode is axisymmetric; whereas, in the third case, the second mode is axisymmetric. Moreover, Table 2 indicates that for all three shells considered, the eigenvalues for the symmetric and antisymmetric motions corresponding to the same value of n (for $n > 0$) do not differ by more than 20%. This was also observed for the buckling loads of unstiffened toroidal shells in Ref. 6. Furthermore, as in the case of cylindrical shells,[13] the results indicate that as the thickness to radius ratio (ζ) is increased, the frequency increases. The value of the frequency parameter approximately doubles when ζ is doubled. Moreover, the results presented in Table 2 indicate that when the radii ratio (η) decreases, all the eigenvalues studied increase, except those corresponding to the axisymmetric mode which decrease.

The effect of the radii ratio on the eigenvalues for $n = 2$, 3, 4, and 5 is shown in Fig. 4 for both the symmetric and antisymmetric motions. The curves indicate that as η decreases, the eigenvalues increase in value. For a particular value of $n > 0$, a decrease in η indicates that the half wavelength around the circumference of the toroidal shell becomes smaller. It is anticipated, that for large values of η, the motion of each toroidal segment between two adjacent modes on the circumference of toroidal shells will be analogous to the motion of cylindrical shells. In the case of circular cylindrical shells[13] the frequency increases as the length of the shell decreases, hence, the frequency of the toroidal shells will increase as η decreases. Moreover, the results in Fig. 4 indicate that for values of η greater than 5, the eigenvalues vary in a nearly linear fashion.

In Figs. 5 and 6, the first four mode shapes of the three toroidal shells considered are presented. In Fig. 5, the symmetric modes are illustrated whereas, in Fig. 6, the antisymmetric modes are

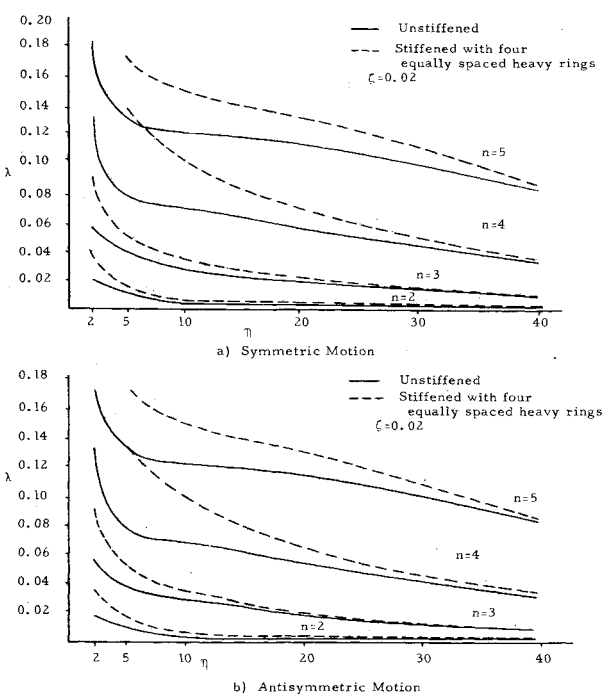

Fig. 4 Frequencies of unstiffened and stiffened toroidal shells vs radii ratio.

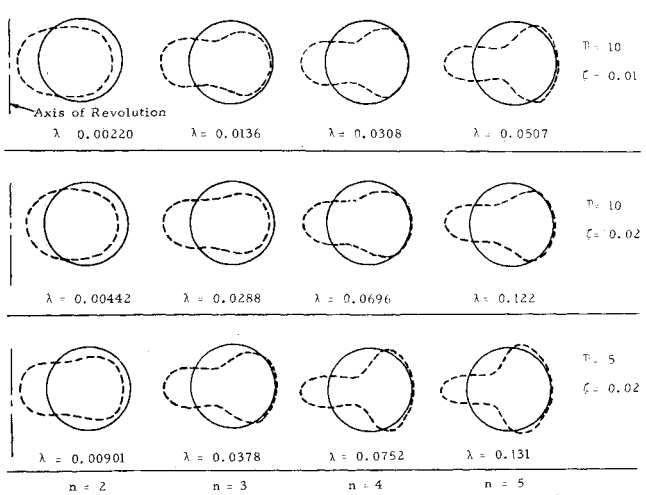

Fig. 5 Symmetric mode shapes of three unstiffened toroidal shells.

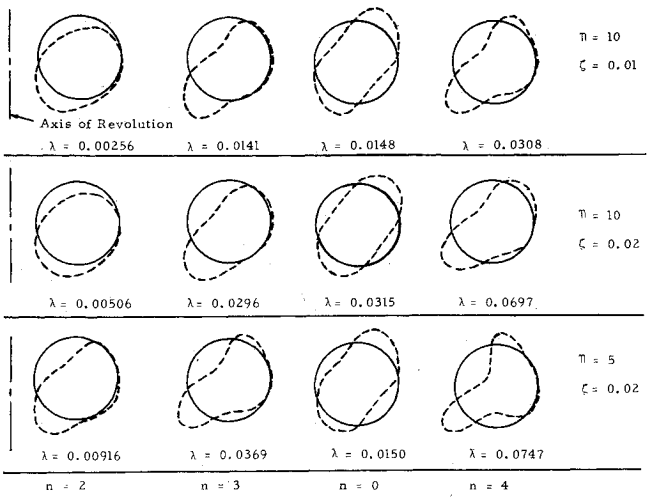

Fig. 6 Antisymmetric mode shapes of three unstiffened toroidal shells.

presented. Both figures show the deformation of the meridional cross section and indicate the number of circumferential harmonics.

Numerical Results for Ring-Stiffened Toroidal Shells

Toroidal shells with $\zeta = 0.02$ and $\eta = 5$ or $\eta = 10$ were considered and the effect on their frequencies and mode shapes of four equally spaced and four unequally spaced rings investigated. Two different types of rings were employed for the cases of equally spaced reinforcement. Their parameters are tabulated in Table 3.

Tables 4–6 give the first five eigenvalues of the symmetric and antisymmetric motions of the stiffened toroidal shells. They also indicate the predominant circumferential harmonic (n) of the motion and give the change $\Delta\lambda$ of the frequency parameter of the stiffened shell from that of the unstiffened shell corresponding to the same circumferential harmonic. Note that generally the frequency increases when the shell is stiffened. As anticipated, the change in the frequency is more appreciable for shells having heavy rings. Moreover, for the same type of rings employed, the change in λ is more appreciable for shells with $\eta = 5$ than with $\eta = 10$. This was anticipated inasmuch as the shapes of the meridional cross sections for the unstiffened shell with $\eta = 5$ are more irregular than those of the shell with $\eta = 10$, and consequently, the rings would exert a greater restriction upon the motion of the shell with $\eta = 5$, than on the motion of a shell with $\eta = 10$ and, hence, they would exert a greater influence on the frequency of the shells with $\eta = 5$.

This effect is further shown in Fig. 4 where the change in the eigenvalues of toroidal shells stiffened with four, equally spaced heavy rings is given for values of η ranging from 2 to 40. The results indicate that the effect of the stiffening rings decreases with increasing η, diminishing to less than 10% for $\eta > 30$ for the modes considered. Moreover, the effect of the rings, generally, is greater for the higher modes, except for low values of η ($\eta < 10$), where the effect of the stiffening rings on the frequency is the greatest for the mode involving predominantly the $n = 4$ circumferential harmonic. In Fig. 4, it is also indicated that the

Table 3 Ring parameters

	$\bar{A}$	$\bar{I}_\psi$	$\bar{I}_z$	$\bar{J}$	$\bar{\Gamma}$	$\bar{\rho}\bar{E}$	$\bar{G}$
1) Light ring	0.005	5×10^{-6}	2×10^{-6}	5×10^{-6}	0	1	$\frac{1}{3}$
2) Heavy ring	0.01	1×10^{-5}	2×10^{-6}	5×10^{-6}	0	1	$\frac{1}{3}$

Table 4 Frequencies of the symmetric motion of a stiffened toroidal shell with four equally spaced rings

$\eta = 10, \zeta = 0.02, \nu = 0.3$

Light rings			Heavy rings		
n	λ	$\Delta\lambda$[a] in %	n	λ	$\Delta\lambda$ in %
2	0.00439	−0.6	2	0.00436	−1.3
2	0.00562	+27.1	2	0.00640	+44.0
3	0.0325	+12.8	3	0.0346	+20.1
4	0.0698	+0.3	4	0.0698	+0.3
4	0.0901	+29.5	4	0.101	+45.1

$\eta = 5, \zeta = 0.02, \nu = 0.3$

Light rings			Heavy rings		
n	λ	$\Delta\lambda$ in %	n	λ	$\Delta\lambda$ in %
2	0.00894	−0.8	2	0.00883	−2.0
2	0.0130	+44.3	2	0.0152	+68.7
3	0.0467	+23.5	3	0.0510	+34.9
4	0.0764	+1.6	4	0.0764	+1.6
4	0.116	+54.2	4	0.135	+79.5

[a] $\Delta\lambda$ is the change in λ due to the presence of the rings.

Table 5 Frequencies of the antisymmetric motion of a stiffened toroidal shell with four equally spaced rings

$\eta = 10, \zeta = 0.02, \nu = 0.3$

Light rings			Heavy rings		
n	λ	$\Delta\lambda$ in %	n	λ	$\Delta\lambda$ in %
2	0.00506	0	2	0.00506	0
2	0.00635	+25.6	2	0.00713	+40.9
3	0.0333	+14.2	3	0.0353	+19.2
0	0.0355	+12.6	0	0.0375	+19.0
4	0.0697	0	4	0.0697	0

$\eta = 5, \zeta = 0.02, \nu = 0.3$

Light rings			Heavy rings		
n	λ	$\Delta\lambda$ in %	n	λ	$\Delta\lambda$ in %
2	0.00917	+0.1	2	0.00914	−0.2
2	0.0131	+43.0	2	0.0152	+65.9
0	0.0183	+22.0	0	0.0205	+36.6
3	0.0458	+24.1	3	0.0498	+34.9
4	0.0760	+1.7	4	0.0758	+0.8

Table 6 Frequencies of the symmetric and the antisymmetric motion of a stiffened toroidal shell with unequally spaced rings

$\eta = 10, \zeta = 0.02, \nu = 0.3$

Symmetric motion with four heavy rings			Antisymmetric motion with four heavy rings		
n	λ	$\Delta\lambda$ in %	n	λ	$\Delta\lambda$ in %
2	0.00481	+8.8	2	0.00548	+8.3
2	0.00583	+31.9	2	0.00649	+28.5
3	0.0325	+12.8	3	0.0317	+7.1
3	0.0361	+25.3	3	0.0354	+19.6
4	0.0697	+0.1	0	0.0427	+35.5

rings alter the frequencies of the symmetric and antisymmetric motion by approximately the same percentage.

Mode shapes for the stiffened shells with $\eta = 10$ are shown in Figs. 7 and 8. They are illustrated by indicating the deformed shape of the meridional section and by depicting the change in the shape around the circumference.

It should be noted that due to the presence of the rings, the deformation changes shape as well as magnitude at different sections around the circumference. In the vicinity of the rings the deformed shape of the meridional sections are more circular in form than at stations away from the rings. In Figs. 7 and 8, only the general form of the deformation is indicated. In Ref. 10 the deformation at several meridional sections is given.

Figure 7 shows the frequencies and mode shapes of the symmetric motion of a toroidal shell with $\eta = 10$, $\zeta = 0.02$ which is stiffened with four, equally spaced heavy rings. The frequency of the first mode is analogous to that of the unstiffened shell, indicating that the predominant circumferential harmonic is the $n = 2$ and that the nodal planes (planes of zero radial displacement) occur at the meridional sections where the rings are located. Thus, in this case, the rings remain essentially undisturbed and, consequently, have a negligible effect upon the motion.

The subsequent mode also involves predominantly the $n = 2$ circumferential harmonic; however, in this mode, the location of the nodes does not coincide with the location of the rings. In point of fact, the maximum radial component of the displacement occurs at the location of the rings. As anticipated, the rings render the deformed shapes of the meridional cross sections of the shell more circular in form.

The third mode involves predominantly the $n = 3$ circumferential harmonic, where two of the stiffening rings experience negligible radial motion, whereas, the other two rings experience the maximum radial motion.

The next mode involves predominantly the $n = 4$ circumferential harmonic with the circumferential nodes located at the four rings. As anticipated, the frequency is analogous to that of the unstiffened shell. The next mode, which is not shown, also has an $n = 4$ shape. However, the rings experience maximum motion and the frequency is higher.

Figure 7 also depicts the frequencies and mode shapes of the antisymmetric motion for the cases previously considered. As illustrated in the figure, the effect of the stiffening rings on the antisymmetric modes is similar to that on the symmetric modes. However, as in the case of the unstiffened shells, an additional mode occurs in the antisymmetric motion which involves predominantly the $n = 0$ harmonic superimposed on the $n = 4$ circumferential harmonic. Thus, for this mode, the rings alter the character of the motion and the coupling of circumferential harmonics is evident.

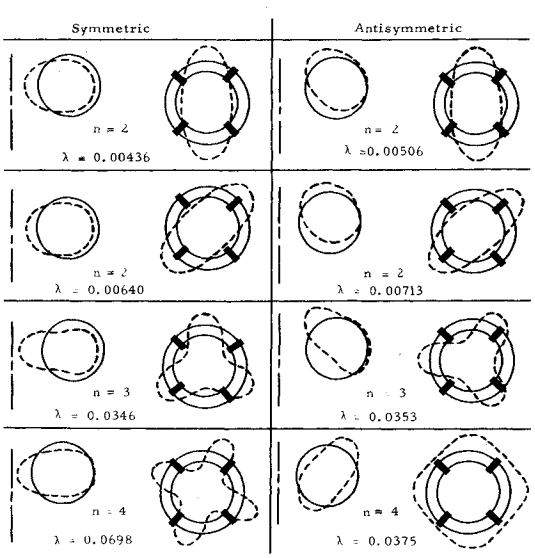

Fig. 7 Mode shapes for first four frequencies of a toroidal shell stiffened with four heavy rings equally spaced $\eta = 10$, $\zeta = 0.02$, $\nu = 0.03$.

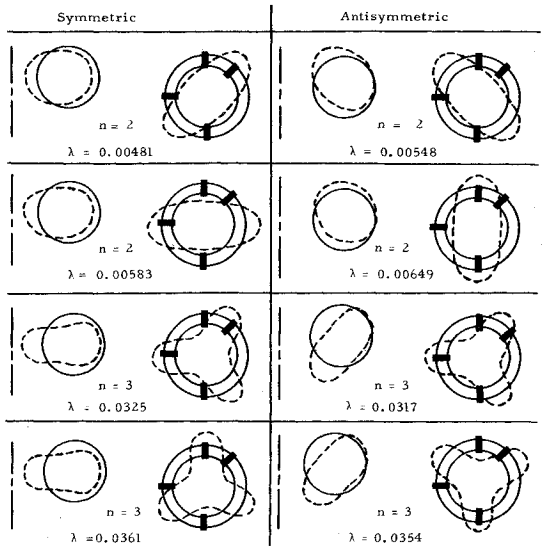

Fig. 8 Mode shapes for first four frequencies of a toroidal shell stiffened with four heavy rings unequally spaced $\eta = 10$, $\zeta = 0.02$, $\nu = 0.3$.

Figure 8 depicts the frequencies and mode shapes of the symmetric and antisymmetric motions of toroidal shells with $\eta = 10$, $\zeta = 0.02$, stiffened with four, unequally spaced, heavy rings. Note that as in the case of shells with equally spaced rings, the first two symmetric and the first two antisymmetric modes involve predominantly the $n = 2$ harmonic. The frequency of the first symmetric and the first antisymmetric mode is higher than that of the unstiffened shell. This is due to the fact that one of the rings does not lie at a nodal section. The two subsequent modes for both symmetric and antisymmetric motion involve predominantly the $n = 3$ harmonic. The frequency of the first $n = 3$ mode is lower than that obtained when the rings are equally spaced, whereas, the frequency of the second $n = 3$ mode is higher.

Conclusions

The problem of the free vibrations of ring-stiffened toroidal shells was formulated and the frequencies together with the corresponding mode shapes were obtained for different shell parameters and varying ring properties. The rings were treated as discrete members which were coupled to toroidal shell segments by imposing compatibility conditions.

In the formulation of the shell equations, it was established that two types of uncoupled modes exist. The first corresponds to motion which is symmetric about the equatorial plane of the torus and the second to motion which is antisymmetric about this plane. Each of these sets of modes is governed by an infinite set of ordinary differential equations which, subsequent to truncation, can be solved by the stepwise integration method with the integration proceeding in the θ direction. This approach yields satisfactory results. Checks of the frequencies of unstiffened toroidal shells with available results concurred to within 2.1%.

A technique for obtaining eigenvalues, originally used in the buckling analysis of rotationally symmetric shells, was also shown to converge very rapidly in the present investigation. This technique has several advantages over conventional methods of obtaining eigenvalues.

The convergence characteristics of the roots of unstiffened toroidal shells were studied as the number of harmonics retained was increased. Plots were established showing the effect of the shell parameters on the number of harmonics that must be retained for three-figure accuracy in the roots. It was found that

more harmonics must be retained for lower values of the radii ratio, η, and for lower values of $\zeta = h/R$.

The five lowest frequencies and their corresponding mode shapes of the symmetric and antisymmetric motion of three different unstiffened shells were determined. It was established, that in all cases, the lowest mode corresponds to motion involving the circumferential harmonic $n = 2$. Moreover, it was established that the frequencies of the symmetric and antisymmetric motion corresponding to the same circumferential harmonic ($n \geqq 2$) did not differ appreciably. The results indicate that the frequency of the unstiffened toroidal shells increased with increasing ζ and decreasing η. The mode shapes for the three different cases considered did not vary appreciably; however, the differences in the frequency were considerable.

When stiffening rings were added to the toroidal shells, the frequencies remained either nearly the same as those of the unstiffened shell (when all the rings occurred along nodal sections) or increased substantially. The changes in the frequencies were greater for the shells with the smaller η. It was established that the stiffening did not alter appreciably the character of the mode shapes. However, in ring-stiffened toroidal shells, the presence of additional modes was established.

References

[1] Sanders, J. L. and Liepins, A. A., "Toroidal Membrane Under Internal Pressure," *AIAA Journal*, Vol. 1, No. 9, Sept. 1963, pp. 2105–2110.

[2] Rossettos, J. N. and Sanders, J. L., "Toroidal Shell Under Internal Pressure in the Transition Range," *AIAA Journal*, Vol. 3, No. 10, Oct. 1965, pp. 1901–1909.

[3] Reissner, E., "On Stresses and Deformations in Toroidal Shells of Circular Cross Section which are Acted Upon by Uniform Normal Pressure," *Quarterly of Applied Mathematics*, Vol. 21, No. 3, Oct. 1963, pp. 177–187.

[4] Liepins, A. A., "Free Vibrations of Prestressed Toroidal Membrane," *AIAA Journal*, Vol. 3, No. 10, Oct. 1965, pp. 1924–1933.

[5] Liepins, A. A., "Flexural Vibrations of the Prestressed Toroidal Shell," CR-296, Sept. 1965, NACA.

[6] Sobel, L. H. and Flügge, W., "Stability of Toroidal Shells Under Uniform External Pressure," *AIAA Journal*, Vol. 5, No. 3, March 1967, pp. 425–431.

[7] Balderes, T. and Armenàkas, A. E., "Free Vibrations of Ring Stiffened Toroidal Shells—Part I Analytical Formulation," PIBAL Rept. 72-12, April 1972, Polytechnic Institute of Brooklyn, Brooklyn, N.Y.

[8] Svalbonas, V. and Armenàkas, A. E. "Linear and Nonlinear Analysis of Shells," PIBAL Rept. 72-20, May 1972, Polytechnic Institute of Brooklyn, Brooklyn, N.Y.

[9] Svalbonas, V. and Balderes, T., "Buckling and Vibration Analysis for Stiffened Orthotropic Shells of Revolution," *AIAA Journal*, Vol. 10, No. 7, July 1972, pp. 944–946.

[10] Balderes, T. and Armenàkas, A. E., "Free Vibrations of Ring Stiffened Toroidal Shells—Part II Numerical Results," PIBAL Rept. 72-22, June 1972, Polytechnic Institute of Brooklyn, Brooklyn, N.Y.

[11] Hurty, W. C. and Rubinstein, M. F., *Dynamics of Structures*, Prentice-Hall, Englewood Cliffs, N.J., 1964.

[12] Sanders, J. L., Jr., "An Improved First-Approximation Theory for Thin Shells," TR R-24, 1959, NASA.

[13] Armenàkas, A. E., Gazis, D., and Herrmann, G., *Free Vibrations of Circular Cylindrical Shells*, Pergamon Press, New York.